Supramolecular Chemistry
Publication details, including instructions for authors and subscription information:
http://www.informaworld.com/smpp/title~content=t713649759

Physicochemical Characterization of Tris(5-acetyl-3-thienyl)methane Inclusion Compounds with 1,*n*-Dichloroalkane Guests (*n*=1 to 10). A Combined TGA, ^{13}C CP/MAS NMR, Powder X-ray Diffraction and DSC Study

Paul S. Sidhu; John A. Ripmeester

To cite this Article Sidhu, Paul S. and Ripmeester, John A.(2003) 'Physicochemical Characterization of Tris(5-acetyl-3-thienyl)methane Inclusion Compounds with 1,*n*-Dichloroalkane Guests (*n*=1 to 10). A Combined TGA, ^{13}C CP/MAS NMR, Powder X-ray Diffraction and DSC Study', Supramolecular Chemistry, 15: 6, 433 — 446

To link to this Article: DOI: 10.1080/1061027031000139349

URL: http://dx.doi.org/10.1080/1061027031000139349

Supramolecular Chemistry, 2003 VOL. 15 (6), pp. 433–446

Physicochemical Characterization of Tris(5-acetyl-3-thienyl)methane Inclusion Compounds with 1,*n*-Dichloroalkane Guests ($n = 1$ to 10). A Combined TGA, ^{13}C CP/MAS NMR, Powder X-ray Diffraction and DSC Study

PAUL S. SIDHU and JOHN A. RIPMEESTER*

National Research Council, Steacie Institute for Molecular Sciences, 100 Sussex Dr, Ottawa, Ontario, Canada K1A 0R6

Received (in Southampton, UK) 20 December 2002; Accepted 8 May 2003

Various physicochemical characterization techniques were used to study tris(5-acetyl-3-thienyl)methane (TATM) inclusion compounds with 1,*n*-dichloroalkane guests ($n = 1$–10). Thermogravimetric analysis (TGA) experiments allowed us to determine host–guest stoichiometric ratios. We determined that the smallest size guests ($n = 1$–4) form 2H:1G TATM inclusion compounds, the intermediate size guests ($n = 5$ and 6) form 3H:1G TATM inclusion compounds, while the largest size guests ($n = 8$–10) form 4H:1G TATM inclusion compounds. From the multiplicity of the host signals in the ^{13}C CP/MAS NMR spectrum, we were able to determine the number of host molecules in the asymmetric unit of each inclusion compound. For $n = 1$–4, there is 1 TATM molecule in the asymmetric unit, for $n = 5$ and 6, there are 3 TATM molecules in the asymmetric unit, while for $n = 8$–10, there are 2 TATM molecules in the asymmetric unit. Powder X-ray diffraction experiments were conducted to determine if any of the nine guests form isostructural TATM inclusion compounds. Only 1,9-dichlorononane and 1,10-dichlorodecane form isostructural TATM inclusion compounds. This behaviour is compared with isostructuralism among previously studied TATM–alkyl halide guest systems. DSC experiments were performed to determine the relationship between the size of guest and the thermal properties of the inclusion compound. We found a direct relationship between the melting temperature and the heat of fusion. These data are compared to a recent study on urea–carboxylic acid complexes.

Keywords: Tris(5-acetyl-3-thienyl)methane; 1,*n*-Dichloroalkane guests; Powder X-ray diffraction; DSC

INTRODUCTION

The tripodal host tris(5-acetyl-3-thienyl)methane (TATM), **1**, is a flexile molecule that can exist in a variety of conformationally isomeric states. It is a host that is similar in structure to the triphenylmethane group of host molecules [1]. It may be prepared by a reaction of chloroform and 2-acetylthiophene, in the presence of the Lewis acid aluminium chloride. When first prepared in 1973, the authors noted that TATM forms inclusion compounds on recrystallization from a small number of solvents [2].

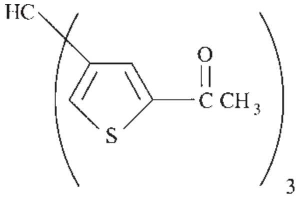

1

In 1977, TATM inclusion compounds with over forty different guests were characterized by their host–guest stoichiometry and melting point [3]. Almost all of the inclusion compounds melted between 80 and 140°C, and most were comprised of a 2:1 host–guest stoichiometric ratio. In addition, the authors were unable to find an organic solvent that would not form a TATM inclusion compound.

---

*Corresponding author. E-mail: jar@ned1.sims.nrc.ca

ISSN 1061-0278 print/ISSN 1029-0478 online
DOI: 10.1080/1061027031000139349

TABLE I Single crystal X-ray diffraction data for TATM inclusion compounds, as reported in the literature [4–12]

Guest	H:G	Lattice	a	b	c	α	β	γ	$V/\text{Å}^3$
Ethyl acetate	2:1	Triclinic ($P\bar{1}$)	8.229	11.229	12.329	99.05	106.40	98.42	1057
Dichloroethane**A**	2:1	Triclinic ($P\bar{1}$)	8.033	10.906	12.306	97.21	106.63	96.69	1011
Ethanol	2:1	Triclinic ($P\bar{1}$)	8.335	10.372	12.488	81.49	71.26	84.95	1010
Cyclohexane**A**	2:1	Triclinic ($P\bar{1}$)	8.622	10.194	12.795	79.09	72.74	84.89	1054
Benzene	2:1	Triclinic ($P\bar{1}$)	11.538	13.560	14.197	89.68	76.60	75.50	2089
CCl_4	2:1	Triclinic ($P\bar{1}$)	11.638	13.684	14.235	88.90	77.46	78.77	2170
Cyclohexane**B**	2:1	Triclinic ($P\bar{1}$)	11.668	13.729	14.227	89.40	77.15	76.24	2157
Cycloheptane	2:1	Triclinic ($P\bar{1}$)	11.721	13.734	14.177	89.22	76.84	76.01	2154
Cyclooctane	2:1	Triclinic ($P\bar{1}$)	11.914	14.013	13.986	89.46	77.15	75.22	2198
Dichloroethane**B**	2:1	Monoclinic ($P2_1/c$)	12.690	12.743	13.737	90	109.05	90	2100
Hexane	3:1	Triclinic ($P\bar{1}$)	12.647	12.694	20.604	85.89	74.31	83.36	3173
Cyclononanone	1:1	Monoclinic ($P2_1/c$)	10.994	19.464	13.417	90	109.40	90	2708

In addition, studies in our own laboratory over the past ten years, involving a very large number of guests, have also failed to reveal a solvent that is not incorporated. In the 1977 study, the authors prepared a variety of TATM analogues, by replacing the acetyl group with other functionalities, such as $OCCH_2CH_3$, $OCCH_2CH_2CH_3$, $OCOCH_3$ and $OCOCH_2CH_3$, among others. Oddly enough, only the methyl ester showed any promise of clathration ability. Finally, attempts at resolving a racemic mixture of 2-butanol on recrystallization from TATM were unsuccessful.

Between 1991 and 2002, single crystal X-ray diffraction data were obtained for TATM inclusion compounds with ten different guests [4–12]. The crystal data appear in Table I. Most are comprised of a 2:1 host–guest stoichiometric ratio, and most crystallize in the triclinic $P\bar{1}$ space group. So far, six different types of crystal lattice are found to occur, based on the unit cell parameters. In all of the structures, the thermal displacement parameters of the guest's atoms are much larger than those of the host's atoms. This suggests either the presence of disorder on the part of the guest molecules or that the guest lattice positions are not fully occupied. In addition, two guests, cyclohexane [11] and 1,2-dichloroethane [12], were found to crystallize with TATM in two different forms, in other words, as a polymorph.

In a previous work [13], we performed a similar physicochemical characterization of TATM inclusion compounds with alkyl halide guests, again using a multi-technique approach. The strategy employed was to study guests with the same hydrocarbon backbone but with different halogen substituents (F, Cl, Br, I) at selected sites on that backbone. From the multiplicities of the host signals in the ^{13}C CP/MAS NMR spectra, the number of TATM molecules in the crystallographic asymmetric unit was determined. Powder X-ray diffraction experiments allowed us to investigate structural isomorphism of TATM inclusion compounds with different guests. In most cases, TATM forms isomorphic structures with guests that have the same hydrocarbon backbone, but with different halogen substituents. This was illustrated in the case of cyclohexyl halide and methylene halide guests. On the other hand, TATM will form one type of structure with a guest that has smaller halogen substituents (e.g. F, Cl, Br), but a completely different structure with a guest that has larger halogen substituents (e.g. I). This was illustrated in the case of monohalobenzene, 2-halobutane and 1,3-dihalopropane guests. Differential scanning calorimetry experiments allow one to investigate thermal stabilities of inclusion compounds with different guests. The enthalpy of decomposition data show that TATM forms more stable inclusion compounds with guests that have smaller, more electronegative halogen substituents (for a given hydrocarbon backbone), and the stability decreases as the size of the halogen substituent increases.

In this study, we chose to perform a systematic study of guests that contain two chlorine atoms at either end of a hydrocarbon chain, with the length of the chain increasing from 1 carbon (dichloromethane) to 10 carbons (1,10-dichlorodecane). The nine guests studied appear in Fig. 1. We wish to see how the properties of the TATM inclusion compounds change as the length of the hydrocarbon chain of the guest increases. By choosing guests that are similar in structure, we hope to eliminate extraneous complications in the interpretation of our data, the only significant difference between the guests being the length of the hydrocarbon chain in between the two chlorine atoms.

The ^{13}C NMR spectra of solids are dominated by a number of electronic and magnetic interactions [14]. Whereas in solution these chemical shifts are immediately apparent at their isotropic averages, in solids, the anisotropic interactions must be averaged by the combination of magic angle spinning and high power dipolar decoupling. One important feature of high resolution solid state cross polarization/magic angle spinning (CP/MAS) NMR spectroscopy is that nuclei which are normally considered to be chemically equivalent in solution

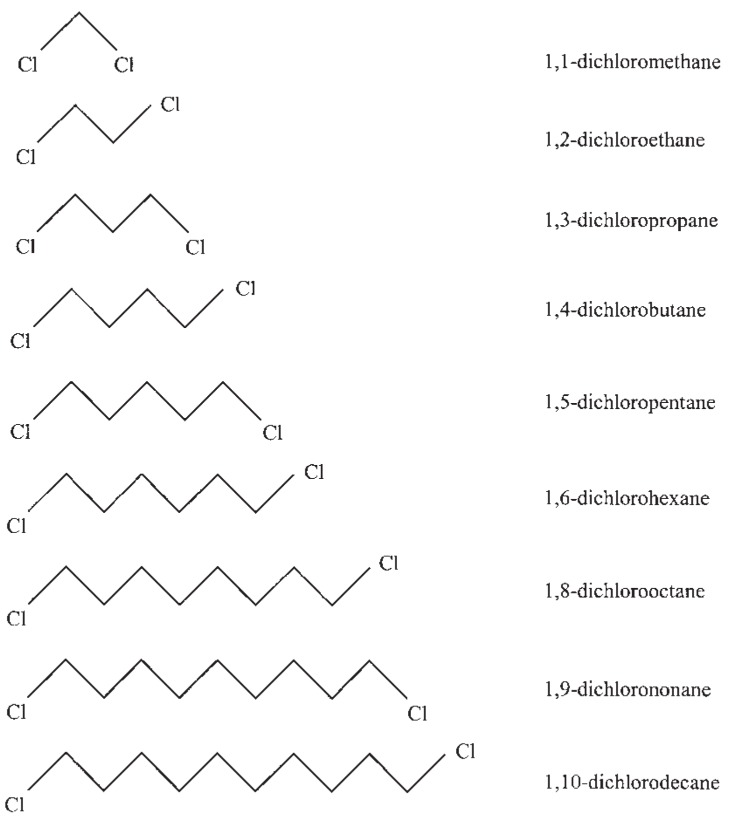

FIGURE 1 The structure of the nine different 1,*n*-dichloroalkane compounds examined as TATM guests in this study.

may not be magnetically equivalent in the solid state, and hence extra signal splittings may occur. In principle, every crystallographically inequivalent atom can give rise to its own resonance. It is the crystallographic symmetry rather than the molecular symmetry that determines the equivalence or non-equivalence of any group of atoms. Examination of the ^{13}C CP/MAS NMR spectrum can therefore give a quick "snapshot" of the contents of the asymmetric unit and has potential as a "fingerprinting" technique for polycrystalline solids.

Powder X-ray diffraction (XRD), as an analytical technique, is useful for confirming the identity of a solid material, determining crystallinity and phase purity, and discovering whether compounds are isostructural based on their respective diffractograms. XRD is also useful as a method for cross-calibrating with the solid-state NMR results to define structure type. Powder X-ray diffraction provides less information than single-crystal X-ray diffraction, however it can characterize the bulk product (rather than a single selected crystal), and can be used on crystalline solids that cannot be prepared as single crystals of sufficient size and quality for conventional single-crystal diffraction studies.

In differential scanning calorimetry (DSC), thermal events in the sample appear as deviations from the baseline, either endothermic or exothermic, depending on whether more or less energy, respectively, is supplied to the sample relative to the reference material [15]. Thus melting points, phase changes, and the associated enthalpies can be determined to give information on the thermodynamic state of the system and relative thermal stabilities.

EXPERIMENTAL

Commercially available reagants (Aldrich) were used as received. (To the best of our knowledge, 1,7-dichloroheptane is not commercially available.) The inclusion compounds were obtained by slow cooling (recrystallization) of hot solutions of 500 mg of the TATM–ethanol inclusion compound in approximately 5 mL of guest solvent, followed by vacuum filtration.

The preparation of TATM proceeded as follows: 2-acetylthiophene (25 g) was added to chloroform (150 g) in a 500 mL round-bottomed flask fitted with a reflux condenser. Anhydrous aluminium chloride (50 g) was added slowly. The mixture was heated at the boiling point of chloroform (61°C) for 1 h, with vigorous stirring. Following this, water and dilute NaOH were added to consume unreacted $AlCl_3$. The chloroform layer was dried with anhydrous $MgSO_4$ and filtered. After evaporating off the chloroform in a rotary evaporator, the remaining viscous oil was crystallized from ethanol. The yield was 13.4 g of the TATM–ethanol inclusion compound, or 52.3% yield, calculated based on the molecular weight of 2 TATM–1 ethanol and 2-acetylthiophene as the limiting reagent.

The ^{13}C CP/MAS NMR spectra were recorded at room temperature on a Bruker AMX 300 NMR spectrometer at a frequency of 75.483 MHz for ^{13}C and 300.145 MHz for ^{1}H. The polycrystalline powder samples were spun in a 5 mm Doty magic angle-spinning (MAS) probe at frequencies between 5 and 6 kHz. The number of scans collected was approximately ten thousand, with 3.8 μs 90° pulses, 5 ms cross polarization contact time, 51.2 ms acquisition time and a 10 s recycle delay. Typically 4096 data points were accumulated with zero filling to 16 K, resulting in a digital resolution of about 2.4 Hz/point. The chemical shifts are given relative to tetramethylsilane at zero ppm, and were referenced externally (by rotor replacement) to the high field signal of hexamethylbenzene (16.9 ppm). Dipolar dephasing experiments were performed by inserting, between the end of cross polarization and the start of ^{1}H decoupled signal acquisition, a short delay (40 μs) with no proton decoupling. This pulse sequence eliminates signals from methine (CH) and methylene (CH_2) carbons, provided they are not reorienting, on the directly bonded $^{13}C-^{1}H$ heteronuclear dipolar coupling timescale.

X-ray powder diffraction patterns (XRD) were recorded at room temperature on a Rigaku Geigerflex vertical goniometer diffractometer with DRX Win 1.3 software, using graphite monochromatized Co-Kα radiation ($\lambda = 1.79$ Å) in the $\theta-\theta$ scan mode. Samples were scanned over a range $10^\circ < 2\theta < 40^\circ$, with a 30 s accumulation time at an increment of 0.02° in 2θ, giving a total acquisition time for each sample of approximately 12 h. We found that this acquisition time was necessary on our instrument to obtain good quality spectra. Voltage and current were set at 30 kV and 20 mA, respectively.

Thermogravimetric analysis (TGA) experiments were performed on a commercial TA Instruments TGA 2050 series system with Thermal Solutions for Windows NT software. Samples of 10 to 20 mg were placed in open aluminium pans and sealed in the furnace. The sample weights were accurate to ± 0.001 mg. Nitrogen was used as a purge gas, flowing at a rate of 40 mL per minute. The samples were heated at a rate of 5°C per minute, from room temperature to about 350°C.

Differential scanning calorimetry (DSC) experiments were performed on a commercial TA Instruments DSC 2920 series system with Thermal Solutions for Windows NT software. Finely powdered specimens, obtained from continuously stirred solutions, were hermetically sealed in aluminium pans, specified to be able to withstand pressures up to five atmospheres. The sample weights were usually between 1–5 mg, and were accurate to ± 0.00001 g. The samples were heated from room temperature to about 250°C, at a rate of 5°C per minute. The samples were purged by a stream of helium flowing at a rate of 40 mL per minute. The calorimeter was calibrated by making a run (at 5°C per minute) with an accurately weighed amount of indium metal, whose heat of fusion is known accurately ($T_m = 156.4°C$, $\Delta H_m = 28.5$ J/g). An empty pan was used for baseline calibration.

RESULTS

Thermogravimetric Analysis (TGA)

TGA experiments were performed on TATM inclusion compounds with the nine different guests depicted in Fig. 1. We wished to determine the stoichiometric ratio (host–guest) for each inclusion compound based on the percent guest loss between room temperature and approximately 225°C. At higher temperatures, the host TATM residue starts to decompose. The TGA curves for the four TATM inclusion compounds with the smallest size guests ($n = 1-4$) appear in Fig. 2. In these plots, the percent guest loss between room temperature and 225–250°C is indicated.

In these plots, one can see two stages of thermal guest loss. Taking 1,3-dichloropropane–TATM (Fig. 2C) as an example, the guest starts to desorb at about 60°C. An initially fast rate of guest loss with respect to temperature, characterized by a steep slope, occurs between 75 and about 100°C. Then, at about 100°C, there is an inflection point in the curve, followed by a much slower rate of guest loss at higher temperatures, characterized by a smaller slope. We believe that this behaviour is related to the change in surface area of the sample when it melts. Before the sample melts at about 100°C, it exists as a polycrystalline powder, with a large effective surface area, so there are more extensive desorption pathways. This results in a large rate of guest loss. On the other hand, after the sample melts, its effective surface area decreases dramatically, as it exists as a molten mass. Therefore the rate of guest loss at higher temperatures occurs much more slowly. This hypothesis is supported by the fact that the TGA inflection point temperatures for all nine inclusion compounds studied here (not shown) correspond very well with the melting temperatures determined by DSC (see "Differential Scanning Calorimetry" Section). For example, the TGA inflection point temperature of 1,3-dichloropropane–TATM is about 100°C, while its DSC melting temperature is about 106°C. The slight difference may be due to the fact that a slight loss of guest in the open TGA pan lowered the melting point below that of the stoichiometric compound.

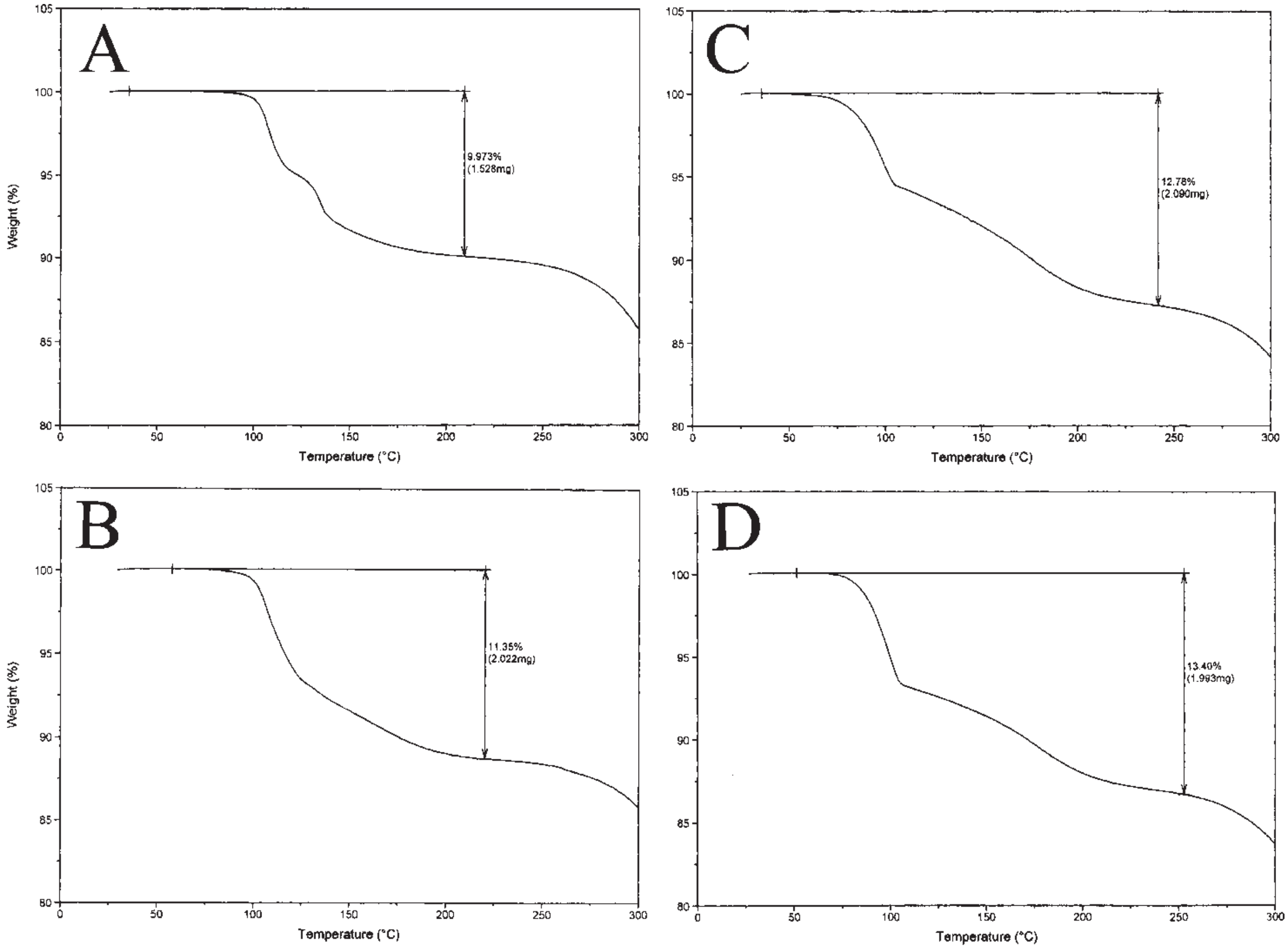

FIGURE 2 TGA curves of the four smallest size 1,*n*-dichloroalkane–TATM inclusion compounds. The percent guest loss between room temperature and ~250°C is indicated on each TGA curve. A: 1,1-dichloromethane–TATM (9.973%); B: 1,2-dichloroethane–TATM (11.35%); C: 1,3-dichloropropane–TATM (12.78%); D: 1,4-dichlorobutane–TATM (13.40%).

In Table II we have compiled the TGA data from all nine inclusion compounds. The experimental percent guest loss for each inclusion compound appears in column 2. In the next five columns, we calculated the expected guest loss for five different host–guest stoichiometric ratios, from 1H:1G to 5H:1G, based on the molecular weights of the guests and TATM. As can be seen in the table, the experimental guest loss for the first four guests ($n = 1-4$) correlates very well with 2H:1G, with no correlation with either 1H:1G or 3H:1G. For the two intermediate size guests ($n = 5$ and 6) the experimental guest loss agrees well with that calculated for a 3H:1G stoichiometric ratio. Finally, for the largest size guests ($n = 8-10$), their experimental guest losses correlate with that calculated for

TABLE II Thermogravimetric data for the nine TATM inclusion compounds with 1,*n*-dichloroalkane guests depicted in Fig. 1

Guest	% Guest loss*	1H:1G†	2H:1G†	3H:1G†	4H:1G†	5H:1G†	S.R.‡
1,1-Dichloromethane	9.97	17.94	**9.85**	6.79			1.97: 1
1,2-Dichloroethane	11.35	20.30	**11.30**	7.83			1.99: 1
1,3-Dichloropropane	12.78	22.53	**12.69**	8.84			1.98: 1
1,4-Dichlorobutane	13.40	24.64	**14.05**	9.83			2.11: 1
1,5-Dichloropentane	10.76		15.36	**10.79**	8.32		3.01: 1
1,6-Dichlorohexane	11.74		16.64	**11.74**	9.07		3.00: 1
1,8-Dichlorooctane	10.84			13.58	**10.54**	8.61	3.88: 1
1,9-Dichlorononane	11.63			14.47	**11.26**	9.21	3.86: 1
1,10-Dichlorodecane	12.56			15.34	**11.96**	9.80	3.78: 1

*The experimental guest loss between room temperature and about 250°C for each inclusion compound, in percent of weight at room temperature. †Calculated percent guest loss for five different stoichiometric ratios, based on the molecular weights of guest and TATM. The closest agreement between calculated and experimental guest loss appears in bold. ‡The exact stoichiometric ratio (to three significant figures) of each inclusion compound, based on the experimental guest loss in column 2.

4H:1G, with no correlation with either 3H:1G or 5H:1G.

In the final column of Table II, we tabulate the exact H:G stoichiometric ratio for each of the nine inclusion compounds to three significant figures, based on the experimental guest loss tabulated in the second column of the table. As can be seen in Table II, the three smallest size guests (dichloromethane, 1,2-dichloroethane and 1,3-dichloropropane) are all within 1% of being exactly 2H:1G. For 1,4-dichlorobutane, however, there is a slight excess of host above and beyond being exactly 2H:1G, about 5%. The two intermediate size guests (1,5-dichloropentane and 1,6-dichlorohexane) form TATM inclusion compounds with a stoichiometric ratio of almost exactly 3H:1G, within 0.3% or less. Finally, the three largest size guests (1,8-dichlorooctane, 1,9-dichlorononane and 1,10-dichlorodecane) form TATM inclusion compounds with a slight excess of guest (between 3.0 and 5.5%), which may perhaps be because these guests, as pure compounds, are fairly involatile. A small amount of guest may be tenaciously sitting freely on the surface of the crystal, refusing to evaporate.

Thus we see the properties of molecular recognition of host for guest during the crystallization process. The smallest size guests ($n = 1-4$) require only two TATM molecules to form the inclusion compound. The intermediate size guests ($n = 5$ and 6) require three TATM molecules to form the clathrate, while the largest size guests ($n = 8-10$) require four TATM molecules to form the inclusion compound. These properties of molecular recognition are further elaborated upon in the next section.

^{13}C CP/MAS NMR

The ^{13}C CP/MAS NMR spectrum of guest-free TATM (prepared by vacuum sublimation) is presented in Fig. 3A. The signals are broad singlets, reflecting the amorphous character of desolvated TATM. For noncrystalline or amorphous solids, the spectral peaks may be broadened as a result of the nuclei having a distribution of electronic environments. In contrast, the ^{13}C CP/MAS NMR signals of TATM in TATM inclusion compounds are usually sharp multiplets, giving information on the crystal symmetry in each case. The NMR signal at lowest field (190.7 ppm) comes from the carbonyl carbon of the acetyl groups of TATM. The signal at highest field (26.4 ppm) originates from the methyl carbon on the same functional group. Both retain their intensity upon dipolar dephasing (Fig. 3B), the latter because of rapid internal methyl rotation. In contrast, the central methine CH host signal at 43.7 ppm is eliminated by this pulse sequence. Finally, the two signals at 132.8 and 145.2 ppm belong to the four thienyl ring carbons. Their assignment is assisted by dipolar dephasing. The quaternary carbons (3 and 5) together give rise to the signal at 145.2 ppm, as they retain their full intensity in Fig. 3B. On the other hand, the signal at 132.8 ppm belongs to the two tertiary CH thienyl carbons (2 and 4). They are eliminated by dipolar dephasing, because of strong heteronuclear one bond ^{13}C–^{1}H dipolar coupling.

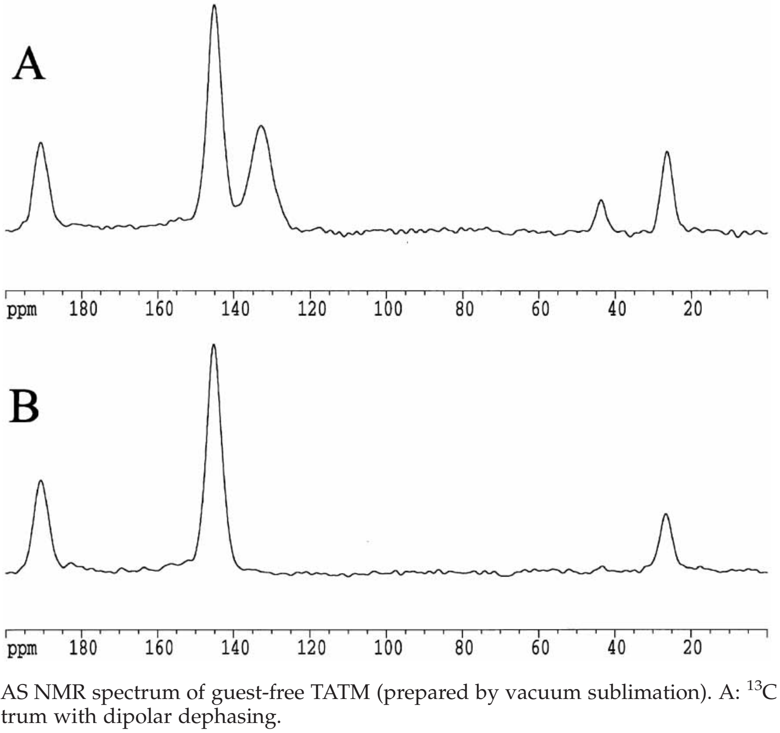

FIGURE 3 The ^{13}C CP/MAS NMR spectrum of guest-free TATM (prepared by vacuum sublimation). A: ^{13}C CP/MAS NMR spectrum; B: ^{13}C CP/MAS NMR spectrum with dipolar dephasing.

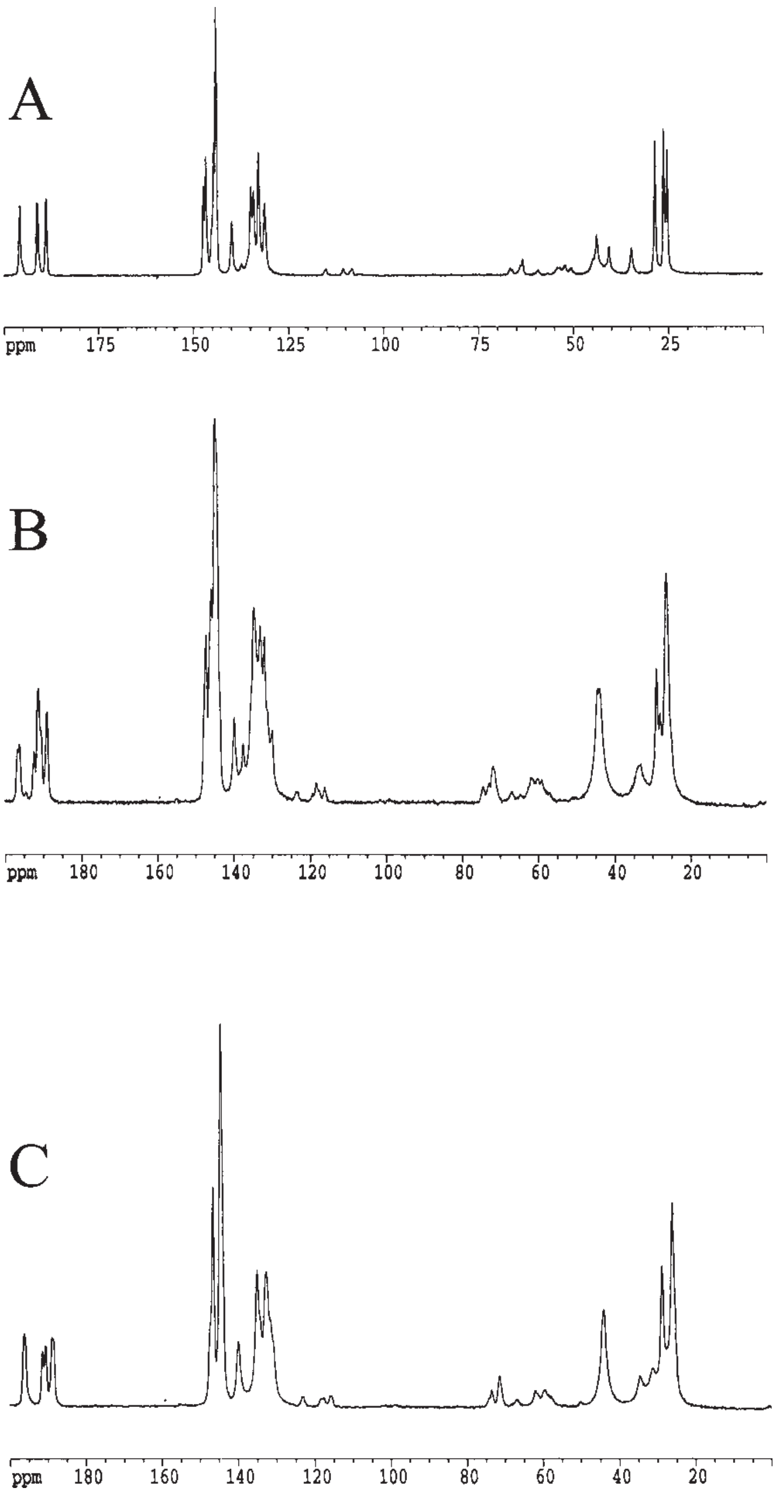

FIGURE 4 ^{13}C CP/MAS NMR spectra of TATM inclusion compounds with three different 1,*n*-dichloroalkane guests. A: 1,3-dichloropropane–TATM; B: 1,5-dichloropentane–TATM; C: 1,9-dichlorononane–TATM.

This experiment also shows that the TATM molecule in guest free TATM (and also in the inclusion compounds) is not reorienting at room temperature, other than internal methyl rotation of the acetyl groups.

The ^{13}C CP/MAS NMR spectra of three selected TATM inclusion compounds appear in Fig. 4. The guests are 1,3-dichloropropane (Fig. 4A), 1,5-dichloropentane (Fig. 4B) and 1,9-dichlorononane (Fig. 4C). For 1,3-dichloropropane–TATM (Fig. 4A), the multiplicity of the host carbonyl signal at 190 ppm is three (three singlets), as is the multiplicity of the host methyl signal at 26 ppm (also three singlets). As there are three carbonyl carbons and three methyl carbons in one host TATM molecule, this implies that there is one TATM

TABLE III ^{13}C CP/MAS NMR data for the nine TATM inclusion compounds with 1,*n*-dichloroalkane guests depicted in Fig. 1

Guest	S.R.*	Host carbonyl multiplicity†	Number of host in A.U.‡
1,1-Dichloromethane	2H:1G	3	1
1,2-Dichloroethane	2H:1G	3	1
1,3-Dichloropropane	2H:1G	3	1
1,4-Dichlorobutane	2H:1G	3	1
1,5-Dichloropentane	3H:1G	9	3
1,6-Dichlorohexane	3H:1G	9	3
1,8-Dichlorooctane	4H:1G	6	2
1,9-Dichlorononane	4H:1G	6	2
1,10-Dichlorodecane	4H:1G	6	2

*Host–guest stoichiometric ratio determined from TGA experiments. †The multiplicity of the TATM host carbonyl signal in each of the nine ^{13}C CP/MAS NMR spectra (see Fig. 4). This signal appears at approximately 190 ppm. ‡The number of host molecules in the asymmetric unit of each TATM inclusion compound, determined from the multiplicity of the host carbonyl signal in column 3 of the table.

molecule in the asymmetric unit. Since the stoichiometric ratio for this inclusion compound is 2H:1G, if one assumes that there are two host molecules and one guest molecule in the unit cell, the two host molecules in the unit cell may be related by a symmetry element (perhaps a centre of symmetry), to give one host molecule in the asymmetric unit. Although not presented in the paper, the three other 2H:1G inclusion compounds also show a multiplicity of three for the host carbonyl and host methyl signals, again suggesting there is one host in the asymmetric unit for these inclusion compounds.

For 1,5-dichloropentane–TATM (Fig. 4B), the multiplicity of the host carbonyl signal at 190 ppm is nine. From lowest to highest field, the individual multiplicities are 2, 1, 4, 2, for a total of nine. The multiplicity of the host methyl signal at 26 ppm is also nine. The individual multiplicities, from lowest to highest field, are 3, 1, 5, for a total of nine. Therefore, this splitting pattern suggests that there are three host molecules in the asymmetric unit of this inclusion compound. The ^{13}C CP/MAS NMR spectrum of the other 3H:1G TATM inclusion compound (1,6-dichlorohexane guest—not included in the paper) also indicates that there are three host molecules in the asymmetric unit of this inclusion compound. One can envisage a situation for these two inclusion compounds where there are three hosts and one guest in the unit cell (3H:1G), with no symmetry elements present. That is, the contents of the unit cell and the contents of the asymmetric unit are equivalent.

Finally, we present the ^{13}C CP/MAS NMR spectrum of one of the 4H:1G inclusion compounds, with 1,9-dichlorononane guest (Fig. 4C). In this case the multiplicity of the host carbonyl signal at 190 ppm is six. From lowest to highest field, the individual multiplicities are 2, 1, 1, 2, for a total of six. The multiplicity of the host methyl signal at 26 ppm is also six, from lowest to highest field the individual multiplicities are 2, 4, for a total of six. Therefore, this splitting pattern suggests that there are two host molecules in the asymmetric unit of this inclusion compound. Although not depicted in this work, the ^{13}C CP/MAS NMR spectra of 1,8-dichlorooctane–TATM and 1,10-dichlorodecane–TATM again suggest that there are two host molecules in the asymmetric unit for both of these inclusion compounds. If there are four hosts and one guest in the unit cell for these three inclusion compounds, one can imagine a situation where there are two pairs of hosts in the unit cell, and each of these two pairs are related by a symmetry element to give two host molecules in the asymmetric unit. In other words, the contents of the asymmetric unit is one-half that of the unit cell.

In Table III we have compiled the ^{13}C CP/MAS NMR data for all nine inclusion compounds studied. On inspection of this table, we again see the properties of molecular recognition of host for guest during the crystallization process. All four of the smallest size guests (2H:1G) crystallize with the same number of host molecules in the asymmetric unit, namely one. In addition, the two intermediate size guests (3H:1G) both crystallize with three host molecules in the asymmetric unit. Finally, all three of the largest size guests (4H:1G) crystallize with two host molecules in the asymmetric unit. Thus we see an important correlation between stoichiometric ratio and the contents of the asymmetric unit for TATM inclusion compounds.

Powder X-ray Diffraction

Our principal goal in performing powder X-ray diffraction studies on these inclusion compounds was to determine if any of the nine inclusion compounds were isostructural. After we performed our TGA and ^{13}C CP/MAS NMR studies on these inclusion compounds, our first inclination was that within each of the three groupings of guest (based on the stoichiometric ratio) we expected to see extensive isostructuralism. This expectation was further fuelled by the fact that within each group, there were the same number of host molecules in

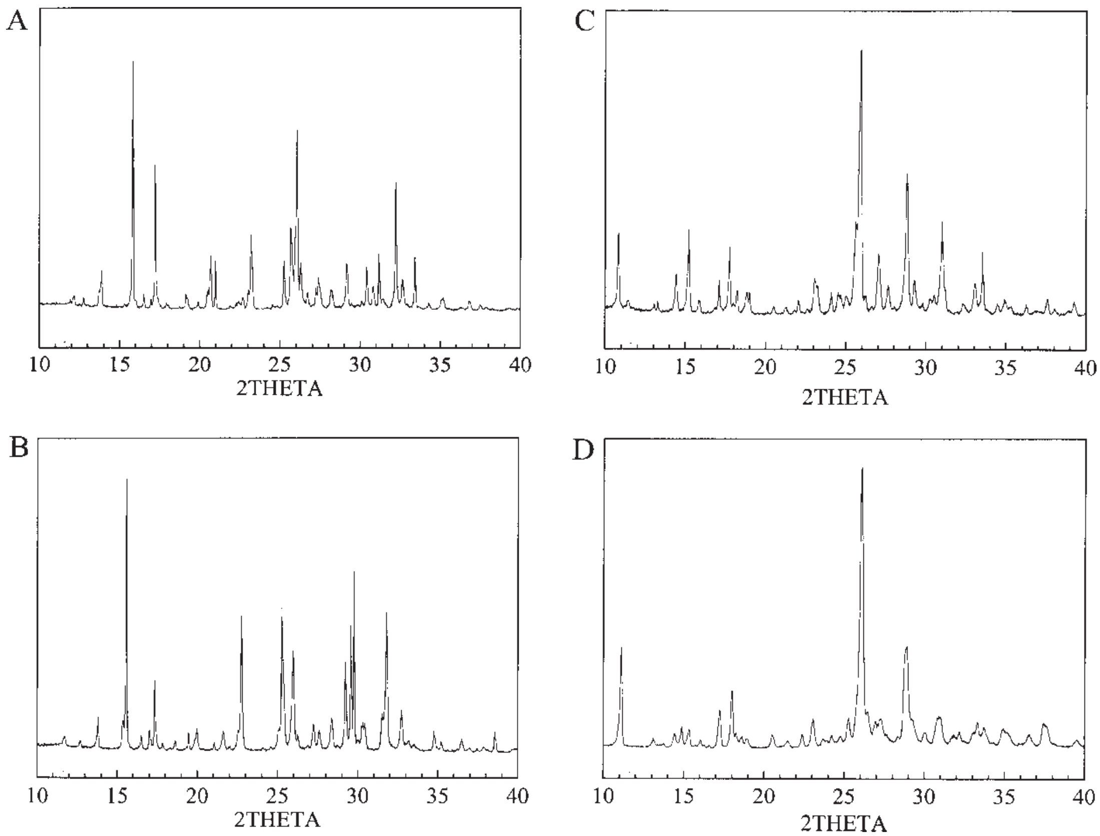

FIGURE 5 Powder X-ray diffraction patterns of TATM inclusion compounds with the four smallest size 1,*n*-dichloroalkane guests. A: 1,1-dichloromethane–TATM; B: 1,2-dichloroethane–TATM; C: 1,3-dichloropropane–TATM; D: 1,4-dichlorobutane–TATM.

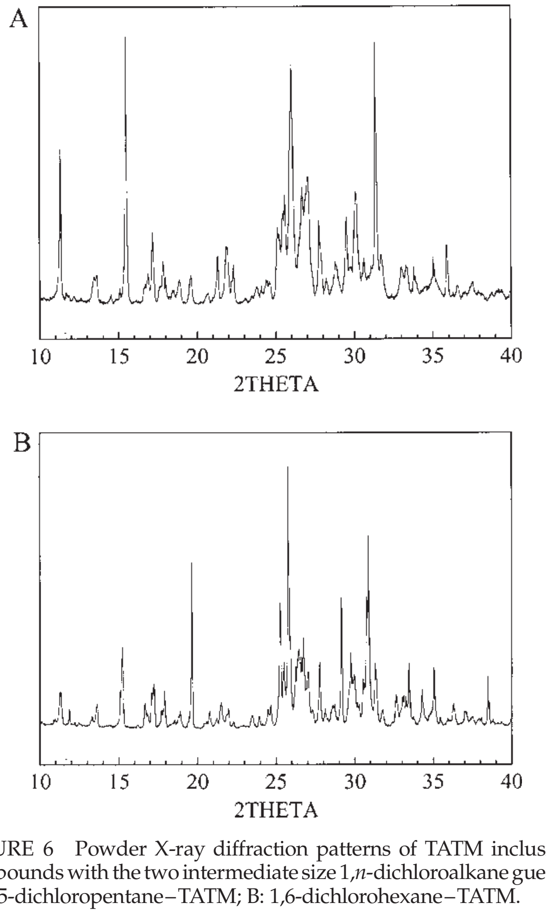

FIGURE 6 Powder X-ray diffraction patterns of TATM inclusion compounds with the two intermediate size 1,*n*-dichloroalkane guests. A: 1,5-dichloropentane–TATM; B: 1,6-dichlorohexane–TATM.

the asymmetric unit of each inclusion compound. However, as we will see, these expectations did not bear fruit.

In Fig. 5, we present the powder X-ray diffraction patterns for the four 2H:1G TATM inclusion compounds ($n = 1$–4). Although some of the patterns share a few common reflections, a detailed analysis of the peak positions indicates that none of the four powder patterns are identical. In other words, none of the four guests form isostructural TATM inclusion compounds. In Fig. 6 is depicted the powder diffraction patterns for the TATM inclusion compounds with two intermediate size guests ($n = 5$ and 6). Again, a detailed analysis of peak positions suggests they are not isostructural. An interesting aside is that, as we previously noted, these two inclusion compounds have three host molecules in the asymmetric unit. This is reflected in the much greater number of reflections for these two inclusion compounds (see Fig. 6) than for either of the other two groups, which have only one or two TATM molecules in the asymmetric unit (see Figs. 5 and 7). Thus we see correlation between the powder X-ray diffraction experiments and the ^{13}C CP/MAS NMR data.

Finally, we present in Fig. 7 the powder diffraction patterns for the three largest size guests, which form 4H:1G inclusion compounds. The diffraction

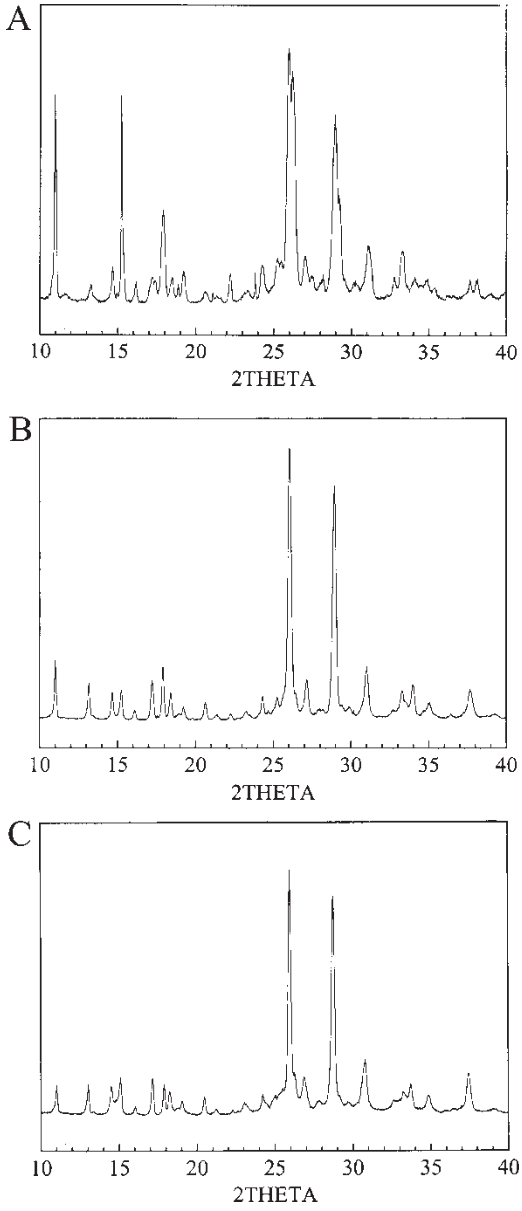

FIGURE 7 Powder X-ray diffraction patterns of TATM inclusion compounds with the three largest size 1,*n*-dichloroalkane guests. A: 1,8-dichlorooctane–TATM; B: 1,9-dichlorononane–TATM; C: 1,10-dichlorodecane–TATM.

patterns for 1,9-dichlorononane–TATM and 1,10-dichlorodecane–TATM are practically identical, with respect to both peak positions and peak intensities. On the other hand, 1,8-dichlorooctane–TATM forms a different type of structure. Thus, for all nine guests, the only ones that are isostructural are 1,9-dichlorononane–TATM and 1,10-dichlorodecane–TATM.

This behaviour can be rationalized by considering the relative percent change in size of the guest on going from an *n*-carbon chain to an $n+1$ carbon chain. In Table IV we tabulate these data, for guests that have the same host–guest stoichiometric ratio. For example, on going from dichloromethane to 1,2-dichloroethane, we are adding one methylene group to a guest that has three backbone atoms (2 Cl and 1 C), so the change in size is $1/3 \times 100$, or 33.3%. For this calculation, we assume that a methylene group and a chlorine atom are roughly similar in size. On the other hand, on going from 1,2-dichloroethane to 1,3-dichloropropane, we are adding one methylene group to a guest that has four backbone atoms, so the relative percent increase in size is $1/4 \times 100$, or 25.0%. At the other extreme, on going from 1,9-dichlorooctane to

TABLE IV Relative percent increase in size of the guest on going from an *n* carbon chain to an $n+1$ carbon chain, for guests that have the same host–guest stoichiometric ratio

Guest	Relative percent size change
1,1-Dichloromethane	
	33.3%
1,2-Dichloroethane	
	25.0%
1,3-Dichloropropane	
	20.0%
1,4-Dichlorobutane	
1,5-Dichloropentane	
	14.3%
1,6-Dichlorohexane	
1,8-Dichlorooctane	
	10.0%
1,9-Dichlorononane	
	9.09%
1,10-Dichlorodecane	

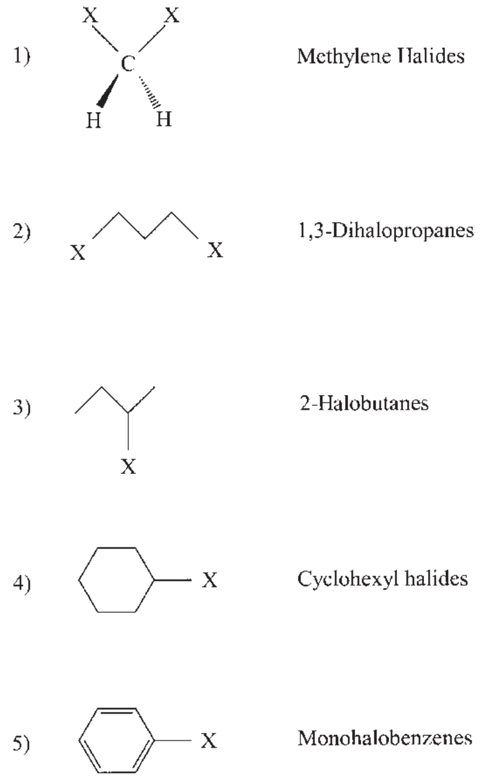

FIGURE 8 Structure of guest molecule families studied as guests in TATM inclusion compounds, in a previous study [13]. X denotes a halogen atom (F, Cl, Br, I).

TABLE V A table of TATM guest families indicating the number of TATM molecules in the respective asymmetric units of each, determined from ^{13}C CP/MAS NMR spectroscopy; additionally, isostructural TATM inclusion compounds are indicated by a common superscript letter. Taken from Ref. [13]

Guest	Number of TATM molecules in the asymmetric unit
Methylene chloride^{a}	1
Methylene bromide^{a}	1
Methylene iodide^{a}	1
1,3-Difluoropropane	1
1,3-Dichloropropane^{b}	1
1,3-Dibromopropane^{b}	1
2-Chlorobutane^{c}	2
2-Bromobutane^{c}	2
2-Iodobutane	2
Benzene^{d}	2
Fluorobenzene^{d}	2
Chlorobenzene^{d}	2
Bromobenzene^{d}	2
Iodobenzene	2
Cyclohexyl chloride^{e}	2
Cyclohexyl bromide^{e}	2
Cyclohexyl iodide^{e}	2

1,10-dichlorodecane, we are adding a methylene group to a guest that 11 backbone atoms, so the relative percent increase in size in $1/11 \times 100$, or 9.09%.

By considering this approach in conjuction with the powder X-ray diffraction results, we can suggest that there is a minimum percent relative increase in size (in our case 9.09%), above which the TATM host can distinguish between two guests that differ in length by one carbon, and subsequently form different structures with these two guests. On the other hand, for percent relative increases in size equal to, or below this value (9.09%), the TATM host cannot distinguish the difference between the size of the two guests, and subsequently forms isostructural TATM inclusion compounds.

These data can be compared with our previous work on TATM with alkyl halide guests. In this work, we investigated isostructuralism, again using powder X-ray diffraction, for these guests. The guest families, depicted in Fig. 8, are the following: methylene halides, 1,3-dihalopropanes, 2-halobutanes, cyclohexyl halides and monohalobenzenes. We systematically varied the halogen substituent(s) (F, Cl, Br, I) on each hydrocarbon backbone to see whether the change in halogen substituent(s) would prompt the TATM host to form a different structure. As summarized in the Introduction, there is extensive isostructuralism within each guest family. Table V compiles these data. Guests that form isostructural TATM inclusion compounds are labelled with a common superscript letter.

Now we can compare the powder X-ray diffraction data for the present study and the previous study. In the previous study, our approach was to choose an invariant hydrocarbon backbone, with varying halogen substituents on that backbone. In the present study, we chose an opposite approach, namely invariant halogen substituents (Cl) with a varying hydrocarbon backbone. There is extensive isostructuralism for the first group, but practically no isostructuralism for the second group. This suggests that during the crystallization process, as far as molecular recognition is concerned, the TATM host cannot distinguish between many of the first group of guests, but can recognize a difference between the guests of the present study. In other words, the effect of systematically changing the size of the hydrocarbon chain has a much greater effect on the size and shape of the guest than does the effect of changing a halogen substituent on a given hydrocarbon framework.

Differential Scanning Calorimetry (DSC)

DSC experiments were performed on TATM inclusion compounds with the nine different guests depicted in Fig. 1. We wished to learn how the melting temperature and the heat of fusion depends on the size of the guest's methylene spacer unit between the two chlorine atoms. The DSC data appear in Table VI. A depiction of the melting endotherms for the TATM inclusion compounds with the four smallest size guests appears in Fig. 9.

The melting temperature is highest for dichloromethane–TATM (134.63°C), rapidly decreases to a minimum for 1,3-dichloropropane (106.46°C), and then gradually increases with the size of guest to reach a local maximum for 1,10-dichlorodecane–TATM (130.89°C). A graph of the dependence of the melting temperature on the carbon chain length of the guest appears in Fig. 10.

The heat of fusion data show a behaviour similar to that of the melting temperature. It is highest for dichloromethane–TATM (41.61 kJ/mol), decreases rapidly to a minimum for 1,3-dichloropropane–TATM (32.37 kJ/mol), and then gradually increases with the size of the guest to reach

TABLE VI Melting temperatures and heat of fusion data for the nine TATM inclusion compounds with 1,n-dichloroalkane guests, determined from differential scanning calorimetric experiments

Guest	T_m (°C)	ΔH_m (J/g)	ΔH_m (kJ/mol TATM)
1,1-Dichloromethane	134.63	107.1	41.61
1,2-Dichloroethane	130.17	103.2	40.10
1,3-Dichloropropane	106.46	83.32	32.37
1,4-Dichlorobutane	109.69	88.72	34.47
1,5-Dichloropentane	117.62	90.85	35.30
1,6-Dichlorohexane	122.07	92.34	35.88
1,8-Dichlorooctane	126.80	94.56	36.74
1,9-Dichlorononane	127.07	95.90	37.26
1,10-Dichlorodecane	130.89	97.33	37.81

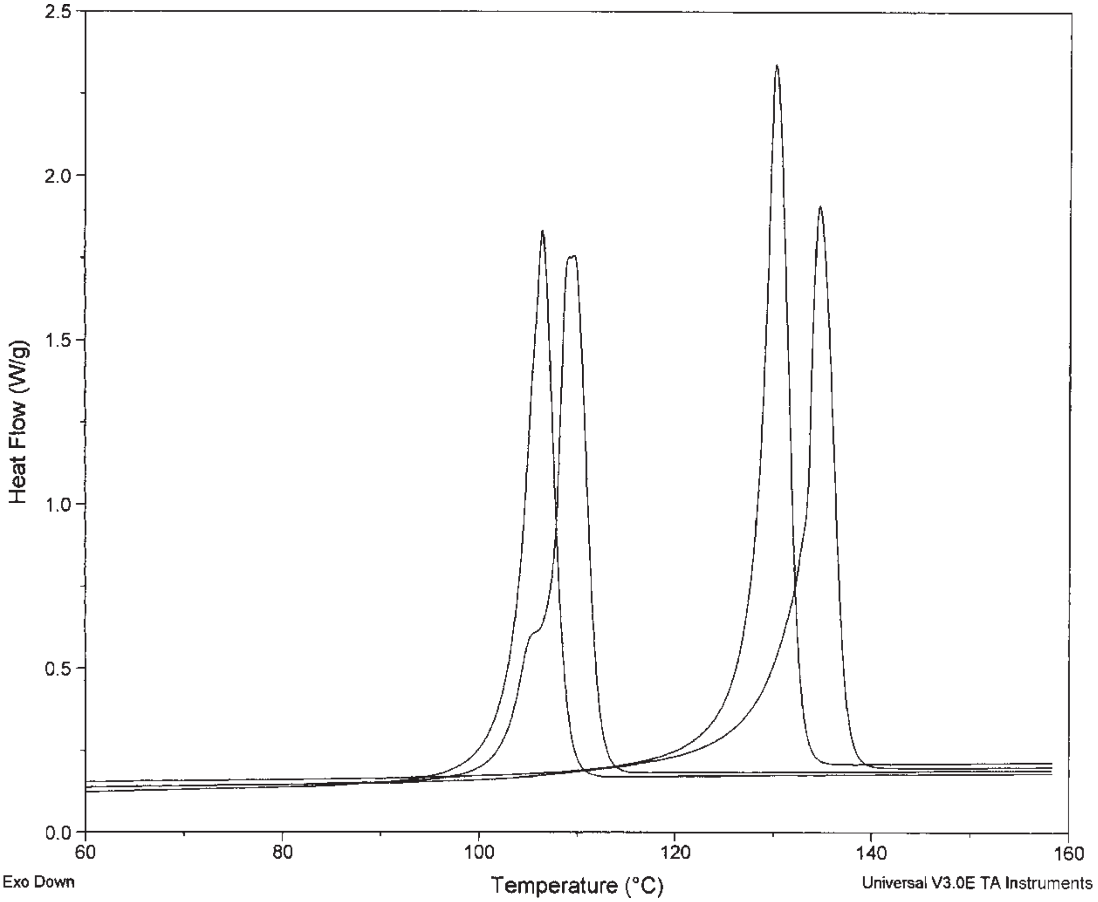

FIGURE 9 DSC melting endotherms for TATM inclusion compounds with the four smallest size 1,*n*-dichloroalkane guests. From lowest to highest temperature, the TATM guests are: A: 1,3-dichloropropane–TATM (T_m = 106.46°C); B: 1,4-dichlorobutane–TATM (T_m = 109.69°C); C: 1,2-dichloroethane–TATM (T_m = 130.17°C); D: 1,1-dichloromethane–TATM (T_m = 134.63°C).

a local maximum for 1,10-dichlorodecane–TATM (37.81 kJ/mol). A graph of the dependence of the heat of fusion on the guest's carbon chain length appears in Fig. 11.

In Fig. 12 is a graph of the heat of fusion plotted against the melting temperature, with a best fit linear regression line. From this graph, one may see that the TATM inclusion compounds with a low melting temperature have a low heat of fusion, the TATM inclusion compounds with a high melting temperature have a high heat of fusion, and TATM inclusion compounds with an intermediate melting temperature have an intermediate heat of fusion.

These results can be compared with a recent publication [16] concerning DSC studies on

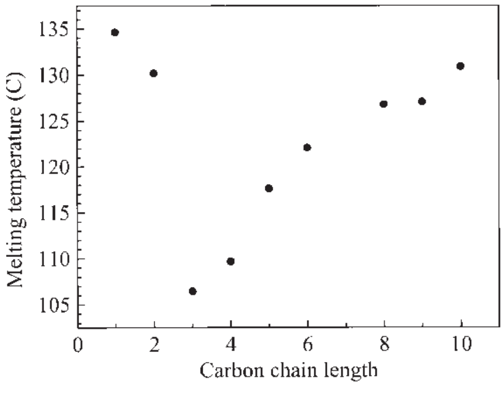

FIGURE 10 A plot of melting temperature against guest carbon chain length for 1,*n*-dichloroalkane–TATM inclusion compounds.

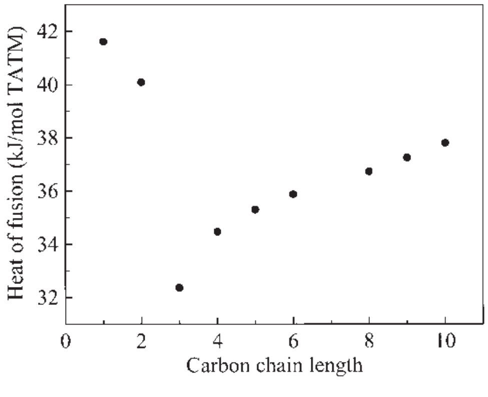

FIGURE 11 A plot of heat of fusion against guest carbon chain length for 1,*n*-dichloroalkane–TATM inclusion compounds.

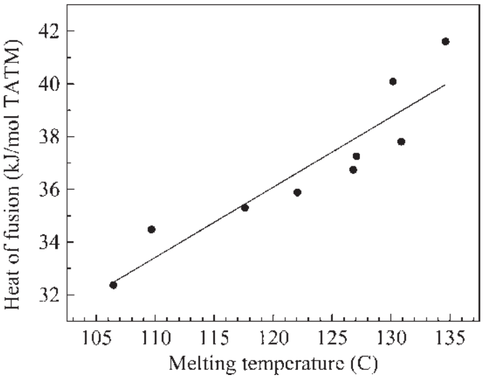

FIGURE 12 A plot of heat of fusion against melting temperature for 1,*n*-dichloroalkane–TATM inclusion compounds, with a best-fit linear regression line.

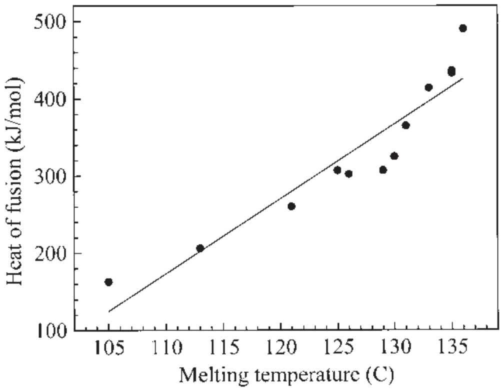

FIGURE 13 A plot of heat of fusion against melting temperature for urea-long chain fatty acid inclusion compounds, with a best-fit linear regression line. The data were taken from Ref. [16].

urea–fatty acid inclusion complexes (C_{10}–C_{30}). In this study, the authors measured host–guest stoichiometric ratios, melting temperatures and heats of fusion for these urea complexes. Their data appear in Table VII. As can be seen in the table, the host–guest stoichiometric ratio increases steadily with the size of guest. They determined the guest acid content by titrating the inclusion compounds against a standard NaOH solution. These data correlate well with our data, in that more host molecules are needed to form the inclusion compound as the size of the guest increases.

The melting temperature and heat of fusion for the urea inclusion compounds both increase steadily with the size of guest, going from a minimum for C_{10} (decanoic acid) ($T_m = 103°\text{C}$, $\Delta H_m = 163\,\text{kJ/mol}$) to a maximum for C_{30} (triacontanoic acid) ($T_m = 136°\text{C}$, $\Delta H_m = 490\text{kJ/mol}$). This agrees partially with the results of our study, with the exception of the two smallest size guests dichloromethane and 1,2-dichloroethane. In Fig. 13 we plot the heat of fusion against the melting temperature for the urea–fatty acid complexes, taken from Ref. [16]. We see a very similar behaviour compared to our results, in that urea inclusion compounds with lower melting temperatures have a smaller heat of fusion, while urea inclusion compounds with higher melting temperatures have a larger heat of fusion.

TABLE VII Host–guest stoichiometric ratios, melting temperatures and heat of decomposition data for urea–fatty acid inclusion compounds (data taken from Ref. [16])

Acid guest	H:G ratio	T_m (°C)	ΔH_m (kJ/mol)
Decanoic acid (C_{10})	8.18:1	105	163
Dodecanoic acid (C_{12})	9.76:1	113	206
Tetradecanoic acid (C_{14})	11.0:1	121	260
Hexadecanoic acid (C_{16})	12.2:1	125	307
Heptadecanoic acid (C_{17})	13.8:1	126	302
Octadecanoic acid (C_{18})	14.2:1	129	307
Eicosanoic acid (C_{20})	14.5:1	130	325
Docosanoic acid (C_{22})	15.6:1	131	365
Tricosanoic acid (C_{23})	17.1:1	133	414
Tetracosanoic acid (C_{24})	18.8:1	135	433
Octacosanoic acid (C_{28})	23.7:1	135	436
Triacontanoic acid (C_{30})	25.4:1	136	490

FURTHER WORK

We have obtained a series of 1-bromoalkane guests, $Br(CH_2)_nCH_3$ ($n = 1$–15). We wish to perform similar experiments with this group of TATM inclusion compounds, such as TGA, DSC, powder X-ray diffraction and ^{13}C CP/MAS NMR. It is hoped that these studies will shed further light upon the present work.

SUPPLEMENTAL MATERIAL

For each of the nine powder X-ray diffraction patterns, tables of reflection angles (2θ) and percent intensities relative to the most intense peak for each reflection have been deposited as supplemental material.

Acknowledgements

The authors are grateful to Natural Sciences and Engineering Research Council of Canada (NSERC) for financial support, in the form of a post-graduate scholarship to P. S. and an operating grant to J. R. In addition, P. S. was the recipient of an Ontario Graduate Scholarship (OGS).

References

[1] Hartley, H.; Thomas, N. G. *J. Chem. Soc.* **1906**, *89*, 1013.

[2] Yakubov, A. P.; Sudarushkin, Y. K.; Belen'kii, L. I.; Gol'dfarb, Y. L. *J. Org. Chem. (USSR)* **1973**, *9*, 1549.

[3] Bin Din, L.; Meth-Cohn, O. *J. Chem. Soc., Chem. Commun.* **1977**, *21*, 741.

[4] Marsh, R. E. *Acta Crystallogr.* **1994**, *B50*, 112.

[5] Van Rooyen, P. H.; Roos, H. M. *Acta Crystallogr.* **1991**, *C47*, 2468.

[6] Dillen, J. L. M.; Roos, H. M. *Acta Crystallogr.* **1992**, *C48*, 2229.

[7] Roos, H. M.; Dillen, J. L. M. *Acta Crystallogr.* **1992**, *C48*, 1882.

[8] Van Rooyen, P. H.; Roos, H. M. *Acta Crystallogr.* **1991**, *C47*, 2718.

[9] Pang, L.; Hynes, R. C.; Whitehead, M. A. *Acta Crystallogr.* **1994**, *C50*, 615.

[10] Pang, L.; Brisse, F. *Acta Crystallogr.* **1994**, *C50*, 1947.

[11] Pang, L.; Brisse, F. *Can. J. Chem.* **1994**, *72*, 2318.

[12] Sidhu, P. S.; Enright, G. D.; Ripmeester, J. A.; Penner, G. H. *J. Phys. Chem. B* **2002**, *106*, 8569.

[13] Sidhu, P. S.; Ripmeester, J. A. *J. Supramol. Chem.* **2001**, *1*, 63.

[14] Ripmeester, J. A.; Ratcliffe, C. I. In *Comprehensive Supramolecular Chemistry*; Atwood, J. L., Davies, J. E. D., MacNicol, D. D. and Vogtle, F., Eds.; Elsevier Science Ltd.: New York, 1996; Vol. 8, p 323.

[15] White, M. A. In *Comprehensive Supramolecular Chemistry*; Atwood, J. L., Davies, J. E. D., MacNicol, D. D. and Vogtle, F., eds.; Elsevier Science Ltd.: New York, 1996; Vol. 8, p 179.

[16] Ahmad, J.; Freestone, A. J.; Hussain, A. *J. Incl. Phenom. Mol. Recognit. Chem.* **1994**, *18*, 115.